IOSR Journal of Environmental Science, Toxicology and Food Technology (IOSR-JESTFT)
e-ISSN: 2319-2402, p- ISSN: 2319-2399.Volume 20, Issue 11 Ser. II (November 2026), PP 01-06
www.iosrjournals.org

Methylene Blue Adsorption on Raw and Activated Clay from Lubumbashi (Dr Congo): Characterization, Kinetics, Thermodynamics and Critical Reassessment of Isotherm Modeling

JOSEPH KILWA LENGE[1], JEAN-CLAUDE CALEB MUZOMWE[2]

Abstract. *Cationic dyes such as methylene blue (MB) are persistent pollutants of textile and tannery effluents, and local clays are attractive low-cost adsorbents for sub-Saharan Africa. A natural clay from the Katanga Clay Manufactory (KCM) deposit, Lubumbashi, Democratic Republic of the Congo, was used raw (AB), thermally activated at 850 °C (AT), or activated with (10 N) H_3PO_4 (AP) or (10 N)H_2SO_4 (AS). The clay is smectite-rich ($SiO_2/Al_2O_3 \approx 3.2$; plasticity index 24.7%; cation exchange capacity 83.4 meq/100 g), and its specific surface area increased from 131.1 m^2/g (AB) to 146.3 m^2/g (AS). In batch tests (100 mL, 0.6 g adsorbent, 25 mg/L MB), removal reached 91.8–93.0% after 48 h, in the order AB < AT < AP < AS. Nonlinear regression of the kinetic data favoured the pseudo-second-order model only for AS, whereas the pseudo-first-order model described AB, AT and AP equally well or better. Adsorption was endothermic ($\Delta H°$ = 10.7–31.2 kJ/mol) and entropy-driven, and spontaneous over 299–333 K only for AS. Equilibrium data were almost linear between 15 and 50 mg/L (Freundlich n = 0.94–1.20), and the measured uptake (up to 7.5 mg/g) exceeded the Langmuir capacities previously obtained by linearization (4.15–5.13 mg/g), which are therefore not retained. A wider concentration range is required before maximum capacities can be reported. H_2SO_4-activated clay is the most effective adsorbent of the series.*

Keywords: *clay; methylene blue; adsorption; kinetics; nonlinear regression; Lubumbashi.*

Date of Submission: 08-11-2026 Date of Acceptance: 18-11-2026

I. INTRODUCTION

Synthetic dyes such as methylene blue (MB, $C_{16}H_{18}N_3SCl$, M = 319.85 g/mol) are widely used in the textile, paper, leather and cosmetic industries. When released untreated, they persist in water bodies, reduce light penetration and are toxic to aquatic life. Adsorption on inexpensive mineral materials is one of the most accessible treatment routes in resource-limited settings, because it needs little infrastructure and can rely on local raw materials.

Clay minerals combine a layered structure, a permanent negative surface charge, cation exchange capacity and low cost. Their performance can be modified by calcination, which removes structural water, or by mineral-acid attack, which leaches octahedral cations and creates new porosity and acid sites. Recent studies illustrate the range of clay-based adsorbents. Hydrochloric-acid-activated clays from Côte d'Ivoire removed methyl orange following pseudo-second-order kinetics [1]. A clay/carbon composite derived from spent bleaching earth reached 29.54 mg/g for MB [2]. In Tanzania, calcination followed by H_2SO_4 treatment raised the surface area of Pugu kaolin from 15.36 to 149.61 m^2/g and the removal of Basic Blue 9 from 96.82% to 99.91% [3]. A natural clay from Turkey showed pseudo-second-order uptake of MB with an activation energy of 29.21 kJ/mol, indicating physical adsorption [4]. Moroccan clays have been characterized together with DFT, molecular-dynamics and Monte Carlo simulations [5,6], and agricultural-waste activated carbon from Ethiopia has been applied to MB-laden textile wastewater [7].

The Democratic Republic of the Congo hosts large clay deposits in its mining belt, yet their use for water treatment is poorly documented. A previous master's study of the KCM deposit near Lubumbashi reported removal of MB by raw and activated clay, with isotherm parameters obtained from linearized equations [8].

[1] University of Lubumbashi, Faculty of Sciences and Technology, Department of chemistry and industry, BP 1825, Lubumbashi, DR Congo. E-mail: josephkilwal@gmail.com
[2] University of Kinshasa, Faculty of Sciences and Technology, Department of chemistry, B.P 127 Kinshasa XI, Kinshasa, DR Congo. E-mail: muzomwe@gmail.com

Linearization distorts the error structure of the data, and fitting the untransformed equations is generally preferred [9]. The present work has two aims: (i) to give a verified account of the characterization, kinetics and thermodynamics of MB adsorption on raw and activated KCM clay, and (ii) to re-analyse the kinetic and equilibrium data by nonlinear regression with statistical criteria, in order to test the conclusions drawn from the linearized treatment.

II. MATERIALS AND METHODS

2.1. MATERIALS

The clay was sampled at the KCM site, Kalebuka, Annexe commune, Lubumbashi (11°44′18.8″ S, 27°29′46.9″ E), Haut-Katanga, DR Congo. Samples were taken to a depth of 1.2 m on a 600 m^2 grid with 10 m spacing; more than 30 kg was homogenized and quartered. Methylene blue (pharmaceutical grade) and analytical-grade reagents (EDTA, sodium thiosulfate, HCl, H_2SO_4, H_3PO_4, KI) were used with distilled water. Equipment comprised a handheld X-ray fluorescence (XRF) spectrometer (SciAps), a UV–visible spectrophotometer, a pH meter, an oven, an electric furnace, a Bernard calcimeter and a pycnometer.

2.2. METHODS

2.2.1. Characterization

The raw material was air-dried, sieved, and the fraction below 75 µm was retained. Particle-size distribution was obtained by dry sieving and sedimentation. Specific surface area was estimated by the methylene blue spot test. Atterberg limits were determined according to NF P94-051 and plotted on the Casagrande chart. Oxide composition was measured by XRF on samples dried at 105 °C. The cation exchange capacity (CEC) was determined by the copper–ethylenediamine method, loss on ignition at 850 °C, surface pH on a clay–water suspension, and carbonate content with the Bernard calcimeter.

2.2.2. Activation

Thermal activation (AT) consisted of calcining 200 g of raw clay (AB) at 850 °C for 10 h. For chemical activation, 20 g of clay was stirred (800 rpm, 30 min) in 500 mL of 10 N H_2SO_4 (AS) or 10 N H_3PO_4 (AP), settled, washed with hot distilled water to a rinse pH of 3–4, and dried at 105 °C for 24 h.

2.2.3. Batch adsorption

Experiments used 100 mL of MB solution with magnetic stirring and 6 h of contact unless stated otherwise; residual MB was measured by UV–visible spectrophotometry. The adsorbent dose was varied from 0.4 to 1.5 g at 25 mg/L and 27 °C. Temperature (299, 303, 313, 333 K) was studied at 0.6 g and 25 mg/L. Initial concentration (15, 25, 30, 50 mg/L) was studied at 0.6 g and about 300 K. Contact time (1–48 h) was studied at 0.6 g and 25 mg/L. The amount adsorbed was calculated from the mass balance (Eq. 1), where C_0 and C_t are the initial and time-t concentrations (mg/L), V the volume (L) and m the adsorbent mass (g).

$$q_t = \frac{(C_0 - C_t)V}{m} \tag{1}$$

2.2.4. Data analysis

Kinetic data were fitted by nonlinear least squares to the pseudo-first-order model [10] (Eq. 2) and the pseudo-second-order model [11] (Eq. 3), and the intraparticle diffusion model [12] was used on the original linear plots. Equilibrium data were fitted to the Langmuir [13] (Eq. 4), Freundlich [14] (Eq. 5) and Temkin [15] models. Thermodynamic parameters were obtained from the van't Hoff relation (Eq. 6) with $K_d = q_e/C_e$.

$$q_t = q_e(1 - e^{-k_1 t}) \tag{2}$$

$$q_t = \frac{k_2 {q_e}^2 t}{1 + k_2 q_e t} \tag{3}$$

$$q_e = \frac{q_{max} K_L C_e}{1 + K_L C_e} \tag{4}$$

$$q_e = K_F C_e^{\frac{1}{n}} \tag{5}$$

$$\ln K_d = -\frac{\Delta H^\circ}{RT} + \frac{\Delta S^\circ}{R} \tag{6}$$

Nonlinear fits used SciPy (Levenberg–Marquardt for kinetics; bounded trust-region least squares for isotherms). Models were compared with the coefficient of determination (R^2), the root-mean-square error (RMSE) and the corrected Akaike criterion (AICc); standard errors of the parameters were taken from the covariance matrix. With only seven kinetic points and four equilibrium points per adsorbent, these statistics indicate tendencies rather than formal proof.

III. RESULTS AND DISCUSSION

3.1. RESULTS

3.1.1. Characterization of the raw and activated clay

About 36% of the raw sample (by mass) passed the 75 µm sieve. Sedimentation of this fraction gave 57.4% clay, 27.3% silt, 14.2% fine sand and 1.1% gravel. The Atterberg limits (liquid limit 45.3%, plastic limit 20.6%, shrinkage limit 15.8%, plasticity index 24.7%) indicate an inorganic clay of medium plasticity, and the position on the Casagrande chart points to the smectite (montmorillonite–beidellite) domain. XRF analysis (Table 2) shows SiO_2, Al_2O_3 and Fe_2O_3 as the main oxides, with SiO_2/Al_2O_3 ratios of 2.9–3.3, closer to montmorillonite than to illite.

Table 1. Physicochemical properties of raw (AB) and activated (AT, AP, AS) clay.

Property	AB	AT	AP	AS
Specific surface area (m^2/g)	131.1	142.5	144.4	146.3
Density	2.52	2.40	2.17	2.25
Surface pH	7.3	4.30	3.43	3.08
CEC (meq/100 g)	83.4	82.8	80.5	79.1
Loss on ignition (%)	9.31	–	–	–
Carbonate content (%)	≤ 0	≤ 1	≤ 1	≤ 1

Table 2. Oxide composition of the clays by XRF (wt.%).

Sample	SiO_2	Al_2O_3	Fe_2O_3	MgO	K_2O	CaO	SiO_2/Al_2O_3
AB	55.48	17.08	5.13	0.60	0.48	2.39	3.25
AT	55.61	18.66	5.22	0.43	1.18	2.59	2.98
AP	57.22	18.32	5.31	0.64	0.90	1.34	3.12
AS	54.00	18.50	5.55	0.40	1.17	1.01	2.92

Activation increased the specific surface area in the order AB < AT < AP < AS (131.1 to 146.3 m^2/g, +11%), lowered the density and the surface pH (7.3 to 3.1 for AS) and slightly decreased the CEC (83.4 to 79.1 meq/100 g). The surface areas come from the methylene blue spot test and should be confirmed by nitrogen adsorption (BET). The increase is modest compared with that reported for kaolin [3], which is consistent with a starting material already rich in smectite.

3.1.2. Effect of dose, temperature and initial concentration

In all series the residual MB concentration followed the order AB > AT > AP > AS. Increasing the dose from 0.4 to 1.5 g raised the removal of 25 mg/L MB from 84.0% to 90.9% for AB and from 89.2% to 93.4% for AS. Raising the temperature from 299 to 333 K increased removal from 67.9% to 89.4% for AB and from 90.2% to 93.4% for AS, which indicates an endothermic process and a much weaker temperature dependence for the H_2SO_4-activated clay. At 0.6 g and C_0 = 50 mg/L, the amount adsorbed (Eq. 1) was 6.97, 7.13, 7.25 and 7.46 mg/g for AB, AT, AP and AS.

3.1.3. Adsorption kinetics

After 48 h, 91.8%, 92.1%, 92.3% and 93.0% of the MB was removed by AB, AT, AP and AS, respectively. For AS, 74% was already removed after 1 h, against 40% for AB. The linearized treatment of the earlier study gave R^2 = 0.87–0.94 for the pseudo-first-order model and 0.95–0.98 for the pseudo-second-order model, and the latter was retained [8]. Nonlinear regression gives a more nuanced picture (Table 3, Fig. 1). The pseudo-first-order model describes AB, AT and AP as well as, or slightly better than, the pseudo-second-order model (R^2 = 0.979–0.991 against 0.961–0.978; lower AICc). Only for AS is the pseudo-second-order model clearly preferred (R^2 = 0.955 against 0.693; AICc −32.1 against −18.6), because most of the uptake takes place within the first hour and the first sample was taken at 1 h. The pseudo-second-order rate constant still increases with activation (0.21, 0.27, 0.30, 0.88 g mg^{-1} h^{-1}), and the fitted equilibrium capacities (3.7–4.0 mg/g) are close to the theoretical maximum of 4.17 mg/g for complete removal of 25 mg/L MB by 0.6 g of clay. The qt versus $t^{0.5}$ plots were not linear through the origin; the intraparticle diffusion constants (k_{id} = 0.290, 0.244, 0.225 and 0.120 mg g^{-1} $h^{-0.5}$; boundary-layer constant C = 2.25, 2.54, 2.66 and 3.20 mg/g for AB, AT, AP and AS) indicate that film diffusion and pore diffusion both contribute, and that the film contribution is largest for AS.

Table 3. Nonlinear fits of the kinetic data (C_{0} = 25 mg/L, 0.6 g, 100 mL).

Clay	PFO q_e (mg/g)	PFO k_1 (h^{-1})	PFO R^2	PFO AICc	PSO q_e (mg/g)	PSO k_2 (g mg^{-1} h^{-1})	PSO R^2	PSO AICc
AB	3.72	0.553	0.979	−24.3	4.03	0.205	0.978	−23.9
AT	3.75	0.694	0.982	−26.9	4.03	0.270	0.968	−22.9
AP	3.78	0.742	0.991	−32.3	4.04	0.298	0.961	−22.2
AS	3.72	1.559	0.693	−18.6	3.87	0.875	0.955	−32.1

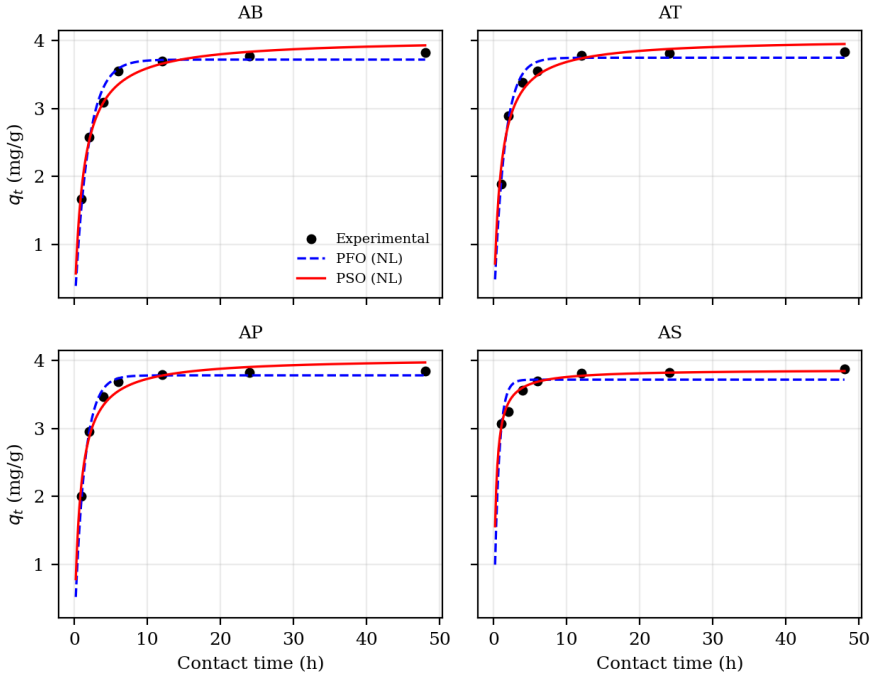


Figure 1. Kinetics of MB adsorption (symbols) with nonlinear pseudo-first-order (PFO) and pseudo-second-order (PSO) fits.

3.1.4. Thermodynamics

The van't Hoff plots reproduce the enthalpies and entropies of the earlier study (Table 4); in that report the ΔH° and ΔS° values of AB and AT were interchanged, and they are corrected here by re-fitting ln K_d against 1/T with the data of the temperature series (R^2 = 0.78, 0.85, 0.92 and 0.99 for AB, AT, AP and AS). All enthalpies are positive and below 40 kJ/mol, and all entropies are positive. The process is therefore endothermic and entropy-driven, and ΔG° is negative from 313 K upwards for AP and over the whole range 299–333 K only for AS. For AB and AT, ΔG° is positive up to 313 K and negative only at 333 K. The weaker temperature dependence of AS (ΔH° = 10.7 kJ/mol) is consistent with its higher uptake at 299 K.

Table 4. Thermodynamic parameters of MB adsorption.

Clay	ΔH° (kJ/mol)	ΔS° (kJ/mol/K)	ΔG° 299 K	ΔG° 303 K	ΔG° 313 K	ΔG° 333 K
AB	27.96	0.088	1.63	1.28	0.39	−1.36
AT	31.20	0.099	1.60	1.20	0.21	−1.77
AP	26.21	0.086	0.50	0.15	−0.71	−2.43
AS	10.70	0.039	−0.96	−1.12	−1.51	−2.29

3.1.5. Equilibrium: reassessment of the isotherm models

The earlier linearized Langmuir treatment gave q_{max} = 4.15, 4.51, 4.93 and 5.13 mg/g (K_L = 0.87–2.70 L/mg; r = 0.992–0.994) [8]. These capacities are lower than the amounts actually adsorbed at C_0 = 50 mg/L (6.97–7.46 mg/g; Table 5, Fig. 2), so they cannot be maximum capacities and could not be reproduced from the C_0–C_e data of that study. Nonlinear regression (Table 5) shows that the Langmuir model is not identifiable for AB, AT and AS: q_{max} runs to the upper bound of the search (10^3 mg/g) with K_L close to zero, and for AP it is 31 ± 35 mg/g. In all four cases the Freundlich exponent is close to unity (n = 0.94–1.20), so that the isotherm is nearly linear over 15–50 mg/L and shows no plateau. The Temkin model fits less well than Freundlich except for AB. Within this range, the data therefore support only a distribution coefficient (K_F), which increases from AB to AS, not a monolayer capacity. By comparison, a smectite-rich natural clay studied up to 500 mg/L reached a Langmuir capacity of 144.93 mg/g [16].

Table 5. Nonlinear isotherm fits (0.6 g, 100 mL, about 300 K) and previous linearized capacities.

Clay	q_e at C_0 = 50 mg/L	Freundlich K_F	Freundlich n	Freundlich R^2	Temkin R^2	Langmuir q_{max} (NL)	q_{max} linearized [8]
AB	6.97	0.75 ± 0.27	0.94 ± 0.17	0.944	0.969	not identifiable	4.15
AT	7.13	0.95 ± 0.07	0.99 ± 0.04	0.997	0.938	not identifiable	4.51
AP	7.25	1.49 ± 0.41	1.20 ± 0.25	0.934	0.903	31 ± 35	4.93
AS	7.46	1.42 ± 0.25	1.00 ± 0.12	0.976	0.960	not identifiable	5.13

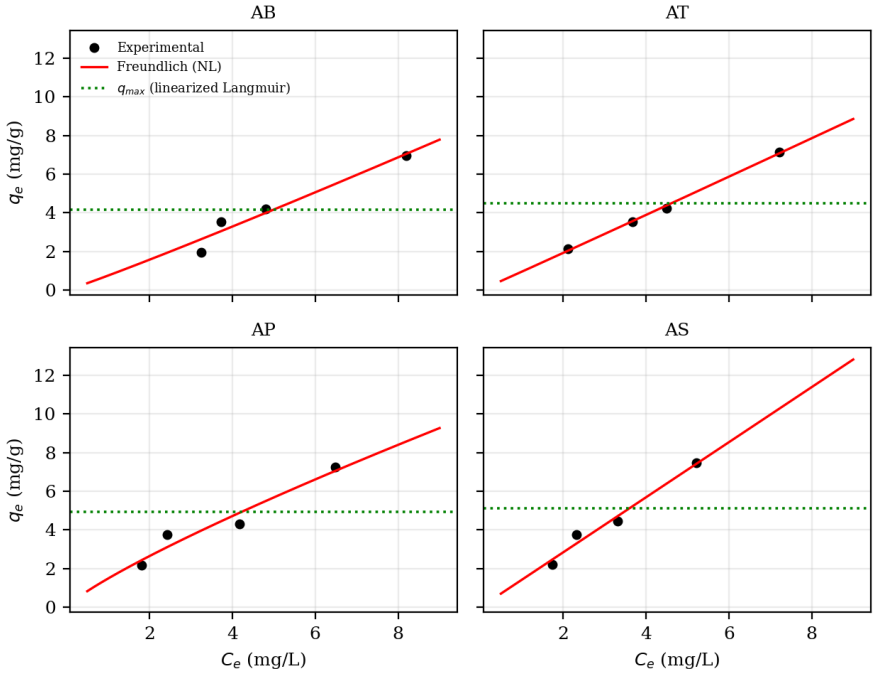


Figure 2. Equilibrium data with nonlinear Freundlich fits; dotted lines show the capacities obtained earlier by linearization.

3.2. DISCUSSION

The consistent order AB < AT < AP < AS in surface area, rate, enthalpy of adsorption and uptake supports the view that acid activation is the most effective treatment of this clay. The CEC decreases slightly with activation while the uptake increases, so exchange capacity alone does not control MB removal; the larger surface area and the modified porosity and acidity are more likely drivers, as is commonly reported for acid-treated clays [3,5]. The positive enthalpies of 10.7–31.2 kJ/mol are in the range of physical adsorption and close to the activation energy found for a Turkish clay [4], whereas much larger values (70–84 kJ/mol) were reported for Moroccan clays [5], so the energetic regime depends on the material and on how K_d is defined. Mechanistic statements here remain tentative, because XRD, FTIR, SEM, BET and point-of-zero-charge data were not available.

Three conclusions of the earlier study are modified by the reassessment. First, the pseudo-second-order model is not uniquely supported; it is preferred for AS, but pseudo-first-order kinetics fit the other three clays equally well. Second, the linearized Langmuir capacities are not retained, and no maximum capacity can be given for this clay at present. Third, the ΔH° and ΔS° values of AB and AT must be interchanged relative to the earlier table. These corrections do not alter the ranking of the adsorbents. The study is limited by single, non-replicated series, a narrow concentration range, sparse early kinetic sampling (first point at 1 h), and the absence of pH-effect experiments. Future work should (i) measure isotherms up to at least 200–500 mg/L with replicates, (ii) sample the first hour of contact densely, (iii) add BET, XRD, FTIR and point-of-zero-charge measurements, and (iv) test real effluents and regeneration.

IV. CONCLUSIONS

Raw clay from the KCM deposit is a smectite-rich material whose capacity to remove methylene blue is improved by thermal activation and, more strongly, by H_3PO_4 and H_2SO_4 activation. After 48 h, 91.8–93.0% of 25 mg/L MB was removed, and the H_2SO_4-activated clay was the fastest and the only adsorbent for which uptake was spontaneous over 299–333 K. Adsorption is endothermic and entropy-driven. Nonlinear regression shows that pseudo-second-order kinetics are clearly preferred only for AS, and that the equilibrium data between 15 and 50 mg/L are nearly linear, so that a Langmuir capacity cannot be established; the capacities of 4.15–5.13 mg/g

previously obtained by linearization are not retained. H_2SO_4-activated clay is the most promising low-cost adsorbent of the series, and measurements at higher concentrations are the next step to quantify its capacity.

Acknowledgement: The authors thank the Department of chemistry and industry, University of Lubumbashi, for access to laboratory facilities.

REFERENCES

[1] Koné, Y. T., Abollé, A., Kambiré, O., Koffi, K. S., Kouadio, K. E., Kimou, K. J., Removal of methyl orange in aqueous media using two clays from Côte d'Ivoire, *Mediterranean Journal of Chemistry*, **15**(1), 2025. https://doi.org/10.13171/mjc02501081810ollo

[2] Madhau, F., Wu, Z., Shi, Y., Wan, D., Tichapondwa, S. M., Wang, Y., Wang, J., Wan, H., Adsorption of methylene blue onto clay/carbon composite: kinetics and isotherms study, *Water Practice & Technology*, **19**(10), 4267, 2024. https://doi.org/10.2166/wpt.2024.237

[3] Erasto, L., Hellar-Kihampa, H., Mgani, Q. A., Lugwisha, E. H. J., Absorbance enhancement of a treated Tanzanian kaolin for removal of synthetic dyes from water, *Tanzania Journal of Engineering and Technology*, **42**(4), 11, 2023. https://doi.org/10.52339/tjet.v42i4.849

[4] Aybar, N., Kul, A. R., Characterization and investigation of natural clay performance for methylene blue removal: results of isotherm, kinetic and thermodynamic studies, *Journal of Elementology*, **29**(4), 1021, 2024. https://doi.org/10.5601/jelem.2024.29.3.3384

[5] Sellak, S., Bensalah, J., Ouaddari, H., Safi, Z., Berisha, A., Draoui, K., Barrak, I., Guedira, T., Bourhia, M., Ibenmoussa, S., Okla, M., Dauelbait, M., Habsaoui, A., Harcharras, M., Adsorption of methylene blue dye and analysis of two clays: a study of kinetics, thermodynamics, and modeling with DFT, MD, and MC simulations, *ACS Omega*, **9**(13), 15175, 2024. https://doi.org/10.1021/acsomega.3c09536

[6] Ouaddari, H., Abbou, B., Lebkiri, I., Habsaoui, A., Ouzzine, M., Fath Allah, R., Removal of methylene blue by adsorption onto natural and purified clays: kinetic and thermodynamic study, *Chemical Physics Impact*, **8**, 100405, 2024.

[7] Fito, J., Abewaa, M., Mengistu, A., Angassa, K., Ambaye, A. D., Moyo, W., Nkambule, T., Adsorption of methylene blue from textile industrial wastewater using activated carbon developed from Rumex abyssinicus plant, *Scientific Reports*, **13**, 5427, 2023. https://doi.org/10.1038/s41598-023-32341-w

[8] Kilwa Lenge, J., Adsorption du bleu de méthylène sur argile brute et activée du gisement de Lubumbashi, Master's thesis (in French), Université de Lubumbashi, Faculty of Sciences, Department of Chemistry, Lubumbashi, DR Congo, 2024.

[9] Kinniburgh, D. G., General purpose adsorption isotherms, *Environmental Science & Technology*, **20**(9), 895, 1986.

[10] Lagergren, S., Zur Theorie der sogenannten Adsorption gelöster Stoffe, *Kungliga Svenska Vetenskapsakademiens Handlingar*, **24**(4), 1, 1898.

[11] Ho, Y. S., McKay, G., Pseudo-second order model for sorption processes, *Process Biochemistry*, **34**(5), 451, 1999.

[12] Weber, W. J., Morris, J. C., Kinetics of adsorption on carbon from solution, *Journal of the Sanitary Engineering Division*, **89**(2), 31, 1963.

[13] Langmuir, I., The adsorption of gases on plane surfaces of glass, mica and platinum, *Journal of the American Chemical Society*, **40**(9), 1361, 1918.

[14] Freundlich, H., Über die Adsorption in Lösungen, *Zeitschrift für Physikalische Chemie*, **57**, 385, 1906.

[15] Temkin, M. I., Pyzhev, V., Kinetics of ammonia synthesis on promoted iron catalysts, *Acta Physicochimica URSS*, **12**, 327, 1940.

[16] Bayar, S., Güneş, A., Taşdemir, A., Adsorption of methylene blue on natural clay: characterization, isotherms, kinetics, and thermodynamics, *Desalination and Water Treatment*, **328**, 101915, 2026. https://doi.org/10.1016/j.dwt.2026.101915